A trans-homologue interaction between reciprocally imprinted *miR-127* and *Rtl1* regulates placenta development.

Mitsuteru Ito[1], Amanda N. Sferruzzi-Perri[2], Carol A. Edwards[1], Bjorn T. Adalsteinsson[1], Sarah E. Allen[1], Tsui-Han Loo[3], Moe Kitazawa[4], Tomoko Kaneko-Ishino[5], Fumitoshi Ishino[4], Colin L. Stewart[3] and Anne C. Ferguson-Smith[1,2]*

[1]Department of Genetics, University of Cambridge, Cambridge CB2 3EH, United Kingdom

[2]Centre for Trophoblast Research, Department of Physiology, Development, and Neuroscience, University of Cambridge, Cambridge CB2 3EG, United Kingdom

[3]Laboratory of Developmental and Regenerative Biology, Institute of Medical Biology, 8A Biomedical Grove, Immunos, Singapore 138648

[4]Department of Epigenetics, Medical Research Institute, Tokyo Medical and Dental University, 1-5-45 Yushima, Bunkyo-ku, Tokyo 113-8510, Japan

[5]School of Health Sciences, Tokai University, 143 Shimokasuya, Isehara, Kanagawa 259-1193, Japan

*Correspondence: afsmith@mole.bio.cam.ac.uk

afsmith@mole.bio.cam.ac.uk

Phone: +44-1223-333-834

Fax: +44-1223-333-786

KEY WORDS: Genomic imprinting, Rtl1, miR-127, placenta development

SUMMARY

The paternally expressed imprinted *Retrotransposon-like 1* (*Rtl1/Peg11)* is a retrotransposon-derived gene that has evolved a function in eutherian placentation. Seven miRNAs, including *miR-127*, are processed from a maternally expressed *antisense Rtl1* transcript (*Rtl1as*) and regulate *Rtl1* levels through RNAi-mediated post-transcriptional degradation. To determine the relative functional role of *Rtl1as* miRNAs in *Rtl1* dosage, we generated a mouse specifically deleted for *miR-127*. The *miR-127* knockout mice exhibit placentomegaly with specific defects within the labyrinthine zone involved in maternal-fetal nutrient transfer. Although fetal weight is unaltered, specific *Rtl1* transcripts and protein levels are increased in both the fetus and placenta. Phenotypic analysis of single (Δ*miR-127/Rtl1* or *miR-127/ΔRtl1*) and double (Δ*miR-127/ΔRtl1*) heterozygous *miR-127* and *Rtl1* deficient mice indicate that *Rtl1* is the main target gene of *miR-127* in placental development. Our results demonstrate that *miR-127* is an essential regulator of *Rtl1* mediated by a trans-homologue interaction between reciprocally imprinted genes on the maternally and paternally inherited chromosomes.

INTRODUCTION

Mammalian genomic imprinting is an epigenetic process whereby genes are mono-allelically expressed in a parent-of-origin specific manner (Ferguson-Smith, 2011). The imprinted gene cluster on mouse chromosome 12 contains four paternally expressed protein-coding genes and maternally expressed non-coding RNAs (Fig. 1A) (da Rocha et al., 2008). One of these paternally expressed genes, *Retrotransposon-like 1* (*Rtl1/Peg11*) is derived from a Ty3/gypsy type retrotransposon that, in eutherians has evolved a large conserved ORF but has lost its

long terminal repeats (LTRs) resulting in loss of original retroviral promoter activity.

(Brandt et al., 2005; Youngson et al., 2005; Edwards et al., 2008).

The primary *Rtl1as* is exclusively expressed from the maternally inherited *Rtl1* locus but in the opposite direction to *Rtl1* (Fig. 1A) (Seitz et al., 2003). At least seven miRNAs processed from *Rtl1as* are therefore 100% complementary in sequence to *Rtl1* (Davis et al., 2005). Maternally inherited deletion of the differentially methylated imprinting control region for the locus (IG-DMR) causes a maternal to paternal epigenotype switch across the whole imprinted gene cluster (Lin et al., 2003). This is associated with repression of all the maternally expressed non-coding RNAs including the miRNAs, and inappropriate activation of the usually paternally expressed protein-coding genes on the maternally inherited chromosome resulting in a double dose. However, *Rtl1* mRNA levels increase 4.5 fold from both alleles, instead of the double dose expected from loss of imprinting (LOI). This suggests that the increase in *Rtl1* dosage in the mutant is the cumulative effect of both LOI and a failure to destabilize the now biallelically expressed transcript by the antisense miRNAs (Lin et al., 2003). Further evidence that these miRNAs can degrade *Rtl1* transcripts by the RNAi machinery *in vivo* came from the identification of both DROSHA and DICER cleavage products for each of the miRNAs (Davis et al., 2005). Previous work has shown that *Rtl1* gene deletion causes growth retardation of both the fetus and placenta and that removal of six of the seven miRNAs on *Rtl1as,* leads to *Rtl1* overproduction and placentomegaly (Sekita et al., 2008).

Further findings indicate that *miR-127* on *Rtl1as* can be independently regulated in human cancer (Iorio et al., 2005; Lu et al., 2005), and that on its own *miR-127* may be the major contributor to *Rtl1* silencing in differentiating mouse embryonic stem (ES) cells (Ciaudo et al., 2009). These findings suggest that *miR-127*

may play a prominent role controlling *Rtl1* dosage during normal development. In order to clarify the biological significance of *miR-127*, we generated *miR-127* knockout mice and studied its impact on *Rtl1* transcript and protein levels and for placental development.

RESULTS AND DISCUSSION

Maternal *miR-127* deletion induces placentomegaly

The schematic organization of the imprinted *Rtl1* sense and antisense transcripts is shown in Fig. 1A. A 134bp deletion removed *miR-127* upon maternal transmission (Δ*miR-127*), while the same deletion when paternally transmitted (Δ*Rtl1*) introduces a nonsense mutation in the (3rd) exon of *Rtl1* resulting in premature translation termination of a normally transcribed mutant transcript (Fig. 1A and S1B). Western blotting data showed no detectable RTL1 protein in Δ*Rtl1* conceptuses (Fig. S1G), although *Rtl1* mRNA was stable (Fig. S3A). All phenotypic analyses were carried out on the C57BL6 background unless otherwise indicated.

Placentae were significantly over-grown in Δ*miR-127* mutants, which was first apparent at E16.5; placental weights were 111.6% and 118.5% compared with WT at E16.5 and E18.5, respectively (Fig. 1B). In contrast, there was no effect of Δ*miR-127* on fetal weight during development (Fig. 1B). Previous work had shown that when six miRNAs, including *miR-127*, are deleted, mutant placental weights are 156% of WT values at E18.5 although fetal weights are not different (Sekita et al., 2008). These data suggest that *miR-127* functions to suppress placental growth in pregnancy, although placentomegaly in Δ*miR-127* was milder than with the larger deletion harboring six miRNAs. After birth the Δ*miR-127* mice grew at comparable rates to

WT and no lethality was observed either pre- or postnatally in these mice (Fig. 1D and Table S1, S2).

Δ*Rtl1* mice showed prenatal growth retardation starting at E16.5; fetal weights were about 80% of WT (Fig. 1C). Mice have reduced wet weight at birth (~70% of WT) and remain growth retarded into adulthood (Fig. 1D). Prenatally, the placenta is growth restricted from E14.5, prior to the onset of fetal growth restriction suggesting a causal role for the placenta in the fetal growth phenotype (Fig. 1C). Prenatal lethality was not observed in Δ*Rtl1* but the majority of neonates died within one day of birth (Table S1 and S2). In situations where Δ*Rtl1* newborns survived more than 2 days, animals survived to adulthood. The lethality of the Δ*Rtl1* was not evident on a mixed 129aa and C57BL/6J background (Table S1). The embryonic lethality we report differs from the previously reported larger deletion, where lethality occurred during gestation upon paternal transmission of the larger deletion (Sekita et al., 2008) despite both mutants lacking the RTL1 protein.

Δ*miR-127* causes defects in the placental labyrinthine zone.

Placental structure was analysed stereologically (Gundersen et al., 1988; Mandarim-de-Lacerda, 2003; Coan et al., 2004) upon both maternal and paternal transmission of the deletion at E18.5. In Δ*miR-127* the labyrinthine zone (Lz), which is the site of nutrient and gaseous exchange between the maternal and fetal blood supplies, was expanded compared to WT (142.3% of WT, Fig. 2A,C). Conversely, the volume of the Lz was reduced in Δ*Rtl1* compared with WT (64.7% of WT, Fig. 2B,D). In contrast to the Lz, the junctional zone (Jz), decidual basalis (Db) and chorion (Ch) were all unaffected by *miR-127* or *Rtl1* deficiency.

Detailed structural analysis of the Lz showed that both the fetal capillaries (FC) and the labyrinthine trophoblast (LT), were significantly increased in Δ*miR-127*, with a non-significant trend for expanded maternal blood spaces (MBS) (Fig. 2E and Fig. S2). Similar to the volume differences, the surface areas of FC and MBS were also extended in Δ*miR-127* (Table S3). Moreover, the average length of FC in the Lz was elongated in Δ*miR-127*, without a change in capillary diameter. There was no effect of *miR-127* deficiency on the thickness of the interhemal trophoblast membrane where nutritional exchange takes place. These results suggest that *miR-127* suppresses fetal capillarisation of the placental exchange region.

In Δ*Rtl1*, placental abnormalities were observed in the same compartments affected by *miR-127* deficiency but with opposite phenotypes (Fig. 2F and Fig. S2). These results suggest that *Rtl1* supports fetal capillary elongation and that the two genes interact to regulate the same placental processes. The alterations in MBS and FC surface area would affect nutrient and oxygen supply to the fetus and contribute to the observed fetal growth restriction. The theoretical diffusion capacity (TDC) and specific diffusion capacity (SDC) are barometers for the potential ability of small molecules like oxygen to transfer by passive diffusion from mother to fetus (Laga et al., 1973). The TDC and SDC values of the mutant placentae indicate that Δ*miR-127* mice have a higher diffusive capacity than WTs and conversely that Δ*Rtl1* placentae have less (Table S3). Although this is likely to contribute to the growth retardation of the Δ*Rtl1* fetuses, it is noteworthy that the Δ*miR-127* mutants are not growth enhanced. Previous work has proposed that *Rtl1* cleaves an extracellular matrix (ECM) component resulting in a release of growth factors to promote hepatocarcinogenesis (Riordan et al., 2013). During angiogenesis, the degradation of the basement membrane and ECM facilitates migration into the interstitial matrix and

formation of new capillaries (Jain, 2003). Since placental Lz RTL1 protein is expressed in the capillary endothelial cells (Sekita et al., 2008), we propose that RTL1 promotes cleavage of the basement membrane to progress the vascularisation of FC.

All *Rtl1* isoforms are regulated by *miR-127*

cDNA screening previously revealed that *Rtl1* had two exons and its transcription start site was located 5 kb upstream of the retrotransposon-like sequences (Hagan et al., 2009) suggesting that *Rtl1* may be regulated by a host-derived promoter outside the retrotransposon. In order to further clarify *Rtl1* transcript structure, we identified further *Rtl1* transcription start sites by 5' RACE. One alternative leader exon was identified in E15.5 placenta (*Rtl Ex1a*) and three alternatives were identified in the E11 embryo (*Rtl1 Ex1b*, *1d* and *1e*), (Fig. 3A and Fig. S4). All five *Rtl1* alternative transcripts including the known *Rtl1 Ex1c* (GeneBank: EU434918), contain a common large exon, namely exon3, which contains the retrotransposon derived ORF, and different small exons. All alternative exon1s are spread over a 12kb region, suggesting they might be transcribed from different promoters. To address this, real time RT-PCR was performed using alternative transcript specific forward primers and a common reverse primer in exon3. This showed that *Rtl1 Ex1c* was the most abundant transcript in E16.5 whole embryos (Fig. S3B). The other *Rtl1* transcripts were also detectable in E16.5 embryos, but *Rtl1 Ex1a* expression level was much lower (0.6%) than the other four. Conversely, the most abundant mRNA in the placenta was *Rtl1 Ex1a* contributing more than 97% of total *Rtl1* expression compared to the others (Fig. S3B).

In order to address whether all *Rtl1* transcripts were equivalently modulated by *miR-127*, we quantified *Rtl1* transcript levels in Δ *miR-127* embryos and placentae. Results showed that all alternative transcripts were significantly over expressed (about 1.7 fold of control) in E16.5 Δ*miR-127* embryos (Fig. 3B). *Rtl1 Ex1a* was significantly increased (1.7 fold) in Δ *miR-127* placentae (Fig. 3B). This is not an indirect effect caused by a disproportionate increase in the number of endothelial cells since there is a similar increase of 70% in *Ex1a* expression when normalized to the endothelial cell marker *PECAM1/CD31* (Fig S3C). Analysis of hybrid fetuses and placentae indicated all alternative transcripts are exclusively transcribed from the paternal chromosome in Δ*miR-127* (Fig. S3D) indicating that the overexpression is not associated with loss of imprinting. Western blotting showed that RTL1 protein was significantly increased proportional to the increased level of the transcript in E16.5 Δ*miR-127* embryos and placentae (Fig. 3C and Fig. S1H). Since deletion of six of the seven miRNAs results in only a 2.5 fold increase of *Rtl1* mRNA (Fig. S3E) our findings indicate that, compared to the other miRNAs in the cluster, *miR-127* contributes a proportionately greater effect on *Rtl1* levels in placentae, and disruption of this repression causes placental over-growth.

Consistent with its impact on *Rtl1* levels, *miR-127* is the most abundant miRNA generated from *Rtl1as* (Fig. 3E). We next determined whether the deletion of *miR-127* influences expression of the neighbouring miRNAs to potentially impact *Rtl1* expression. As expected, *miR-127* was not detected in Δ*miR-127* embryos and placentae (Fig. 3D). In Δ*miR-127* fetuses, only *miR-433-3p* was up-regulated with no change in *miR431*, *miR-434-3p* and *miR-136* expression (Fig. 3D). In contrast, all four miRNAs were significantly up-regulated, with *miR-433-3p* the most induced in Δ*miR-127* placenta. The same miRNAs that were up-regulated in the placenta in the

Δ*miR-127* mutant were down regulated in Δ*Rtl1* (Fig 3D). Together, these results suggest there may be a compensatory feedback mechanism involving RTL1, acting specifically in the placenta to minimize the impact on *Rtl1* transcript levels. *miR-433* has its own promoter and thus may be more sensitive to this feedback mechanism (Song and Wang, 2008).

Rtl1 is the main target gene of *miR-127* for placenta development

Our data suggests *miR-127* can regulate placental growth through *Rtl1* repression. However, to address the possibility that other target genes of *miR-127* might also contribute to placental development, we generated double heterozygous mice (Δ*miR-127/*Δ*Rtl1*) lacking both *Rtl1* and *miR-127*. If *Rtl1* is the main target of *miR-127* leading to repressed placental growth the Δ*miR-127/*Δ*Rtl1* mutant should show a similar phenotype as Δ*Rtl1*. However, if *miR-127* has other targets contributing to this phenotype, the Δ*miR-127/*Δ*Rtl1* mutant would be expected to have an intermediate phenotype between that seen in Δ*Rtl1* and Δ*miR-127*. The Δ*miR-127/*Δ*Rtl1* mutant mouse embryo and placental weight data show that they are similar to Δ*Rtl1* at E18.5 rather than the Δ*miR-127* (Fig. 4A). Histological analysis also showed that the extent and volume reduction of the placental Lz was the same in both the Δ*miR-127/*Δ*Rtl1* and Δ*Rtl1* (Fig. 2C, 4B). Detailed analysis of the Lz also determined that volumes and surface areas of MBS, FC, LT, FC, TDC and SDC were similarly decreased in Δ*Rtl1* and Δ*miR-127/*Δ*Rtl1* compared with WT (Table S3). In contrast, these volumes were increased in Δ*miR-127*. These striking similarities between Δ*Rtl1* and Δ*miR-127/*Δ*Rtl1* placentae suggest *miR-127* specifically acts upstream of *Rtl1* during placental development. Comparative analysis of the genomic locus between eutherian, metatherian and protherian mammals

suggests that miRNAs on *Rtl1as* evolved in eutherians along with the neofunctionalisation of RTL1 (Edwards 2008). Marsupial mammals lack the microRNAs and have retained only remnants of the Ty3/Gypsy retrotransposon that evolved into Rtl1 in eutherians. Hence it is likely that *Rtl1as* miRNAs evolved as a host defence mechanism to negatively modulate the activity of this retrotransposon-derived gene (Edwards et al.*,* 2008). In particular, the reciprocally imprinted, *miR-127* and *Rtl1* that interact so effectively in trans, co-evolved to regulate placenta development.

Materials and methods

Generation of Δ*miR-127/* Δ*Rtl1* mice

We generated a *miR-127* deletion construct that lacks 134bp incorporating *miR-127* (chr12:109,592,803-109,592,936) (Fig. S1A). The *miR-127* targeting construct was transfected into female 129SV ES cells and clones containing the targeting vector were selected (Fig. S1C-E). After deletion of the neomycin resistance gene (Fig. S1F), targeted ES cells were injected into blastocysts to make chimaeras and germline transmission confirmed. Animals were backcrossed to C57BL/6J for ten generations with consistent growth and viability phenotypes noted after N5 on this genetic background (Table S1). Mice were subsequently maintained on a C57BL/6J genetic background. Additional details are described in the supplementary materials and methods.

Placental histology

Placentae from embryonic day (E)18.5 conceptuses were dissected free of fetal membranes, weighed and bisected mid-sagittally. One half was fixed in 4% paraformaldehyde, paraffin-embedded, sectioned, hematoxylin and eosin stained and gross placental structure analysed. The other half was fixed in 4% glutaraldehyde, resin-embedded, toluidine blue stained and structure stereologically assessed. Analyses were performed using the Computer Assisted Stereological Toolbox (CAST v2.0) program as previously described (Coan et al., 2004).

Rapid Amplification of cDNA Ends (5'RACE) and quantitative RT-PCR

5'RACE was performed using First Choice RLM-RACE (Ambion) following the manufacturer's protocol. 10 μg of total RNA from E11 fetus and E15.5 placenta was used as the starting material.

For real time PCR, total RNA (10 μg) from whole embryos and placenta at E16.5, was DNase-treated with RQ1 RNase-free DNase (Promega). cDNA was synthesized using RevertAid™ H Minus First Strand cDNA Synthesis Kit with random hexamers (Fermentas). Real time RT-PCR assay for *Rtl1* was performed using alternative exon 1 specific forward primers and a common reverse primer on exon3. *TATA box binding protein* (*Tbp)* expression was used as internal control.

For mature miRNA expression, we carried out real time RT-PCR using TaqMan MicroRNA Assays (Applied biosystems). Details are described in the supplementary materials and methods.

Western blotting

Proteins were extracted from E16.5 embryos and placentae using RIPA buffer containing protease inhibitors (Complete, EDTA-free, Roche). RTL1 was detected by anti RTL1 rabbit antibody (YZ2843) created in the Stewart lab, and then normalized by *α-Tubulin* (Sigma-Aldrich, T6199). Further details are described in the supplementary materials and methods.

Author contributions

M.I. and A.F.S. designed the study. M.I., A.N.S.P., C.A.E., L.T.H. and M.K. performed experiments. M.I., A.N.S.P., S.E.A., T.K.I., F.I., C.L.S. and A.F.S. analyzed and discussed the data. M.I., A.N.S.P., B.P.A. and A.F.S. wrote the manuscript.

REFERENCE

Brandt, J., Schrauth, S., Veith, A. M., Froschauer, A., Haneke, T., Schultheis, C., Gessler, M. Leimeister, C. and Volff, J. N. (2005). Transposable elements as a source of genetic innovation: expression and evolution of a family of retrotransposon-derived neogenes in mammals. *Gene*, **345**, 101–111.

Ciaudo, C., Servant, N., Cognat, V., Sarazin, A., Kieffer, E., Viville, S., Colot, V., Barillot, E., Heard, E. and Voinnet, O. (2009). Highly dynamic and sex-specific expression of microRNAs during early ES cell differentiation. *PLoS Genet.*, **5,** e1000620.

Coan, P. M., Ferguson-Smith, A. C., and Burton, G. J. (2004). Developmental dynamics of the definitive mouse placenta assessed by stereology. *Biology of Reproduction*, **70**, 1806–1813.

Da Rocha, S. T., Edwards, C. A., Ito, M., Ogata, T. and Ferguson-Smith, A. C. (2008). Genomic imprinting at the mammalian Dlk1-Dio3 domain. *Trends Genet.* **24,** 306–316.

Davis, E., Caiment, F., Tordoir, X., Cavaillé, J., Ferguson-Smith, A., Cockett, N., Georges, M. and Charlier, C. (2005). RNAi-mediated allelic trans-interaction at the imprinted Rtl1/Peg11 locus. *Curr. Biol.* **15,** 743–749.

Edwards, C. A., Mungall, A. J., Matthews, L., Ryder, E., Gray, D. J., Pask, A. J., Shaw, G., Graves, J. A., Rogers, J., SAVOIR consortium, et al. (2008). The evolution of the DLK1-DIO3 imprinted domain in mammals. *PLoS Biol.* **6,** e135.

Ferguson-Smith, A. C. (2011). Genomic imprinting: the emergence of an epigenetic paradigm. *Nat. Rev. Genet.* **12,** 565–75.

Gundersen, H. J., Bendtsen, T. F., Korbo, L., Marcussen, N., Møller, A., Nielsen, K., Nyengaard, J. R., Pakkenberg, B., Sørensen, F. B., Vesterby, A. et al. (1988). Some new, simple and efficient stereological methods and their use in pathological research and diagnosis. *APMIS* **96,** 379-394

Hagan, J. P., O'Neill, B. L., Stewart, C. L., Kozlov, S. V. and Croce, C. M. (2009). At least ten genes define the imprinted Dlk1-Dio3 cluster on mouse chromosome 12qF1. *PLoS One* **4,** e4352.

Iorio, M. V., Ferracin, M., Liu, C. G., Veronese, A., Spizzo, R., Sabbioni, S., Magri, E., Pedriali, M., Fabbri, M., Campiglio, M. et al. (2005). MicroRNA gene expression deregulation in human breast cancer. *Cancer Res.* **65,** 7065–7070.

Jain, R. K. (2003), Molecular regulation of vessel maturation. *Nat Med.* **9,** 685-693.

Laga, E. M., Driscoll, S. G. and Munro, H. N. (1973). Quantitative studies of human placenta. I. Morphometry. *Biol Neonate.* **23**, 231-259

Lin, S. P., Youngson, N., Takada, S., Seitz, H., Reik, W., Paulsen, M., Cavaille, J. and Ferguson-Smith, A. C. (2003). Asymmetric regulation of imprinting on the maternal and paternal chromosomes at the Dlk1-Gtl2 imprinted cluster on mouse chromosome 12. *Nat. Genet.* **35,** 97–102.

Lu, J., Getz, G., Miska, E. a, Alvarez-Saavedra, E., Lamb, J., Peck, D., Sweet-Cordero, A., Ebert, B. L., Mak, R. H., Ferrando, A. A. et al. (2005). MicroRNA expression profiles classify human cancers. *Nature* **435,** 834–838.

Mandarim-de-Lacerda, C. A. (2003). Stereological tools in biomedical research. *An Acad Bras Cienc.* **75,** 469-486.

Riordan, J. D., Keng, V. W., Tschida, B. R., Scheetz, T. E., Bell, J. B., Podetz-Pedersen, K. M., Moser, C. D., Copeland, N. G., Jenkins, N. A., Roberts, L.

R. et al. (2013). Identification of *Rtl1*, a retrotransposon-derived imprinted gene, as a novel driver of hepatocarcinogenesis. *PLoS Genet*. 9, e1003441.

Seitz, H., Youngson, N., Lin, S. P., Dalbert, S., Paulsen, M., Bachellerie, J. P., Ferguson-Smith, A. C. and Cavaillé, J. (2003). Imprinted microRNA genes transcribed antisense to a reciprocally imprinted retrotransposon-like gene. *Nat. Genet.* **34,** 261–262.

Sekita, Y., Wagatsuma, H., Nakamura, K., Ono, R., Kagami, M., Wakisaka, N., Hino, T., Suzuki-Migishima, R., Kohda, T., Ogura, A. et al. (2008). Role of retrotransposon-derived imprinted gene, Rtl1, in the feto-maternal interface of mouse placenta. *Nat. Genet.* **40,** 243–248.

Song, G. and Wang, L. (2008). MiR-433 and miR-127 Arise from Independent Overlapping Primary Transcripts Encoded by the miR-433-127 Locus. *Plos One* **3,** e3574

Wang, H., Riha, G. M., Yan, S., Li, M., Chai, H., Yang, H., Yao, Q. and Chen, C. (2005). Shear stress induces endothelial differentiation from a murine embryonic mesenchymal progenitor cell line. *Arterioscler Thromb Vasc Biol.* 25, 1817-1823.
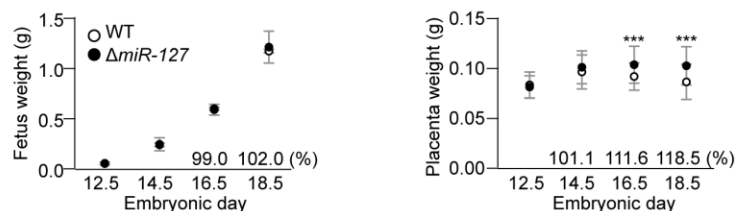
Youngson, N. A., Kocialkowski, S., Peel, N. and Ferguson-Smith, A. C. (2005). A small family of sushi-class retrotransposon-derived genes in mammals and their relation to genomic imprinting. *J. Mol. Evol.* **61,** 481–490.
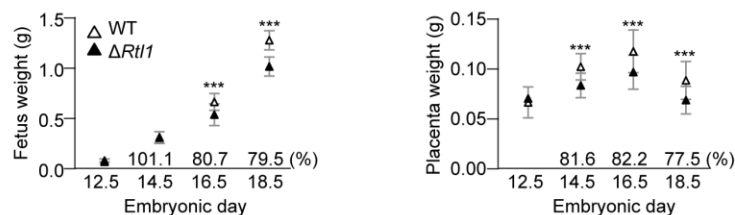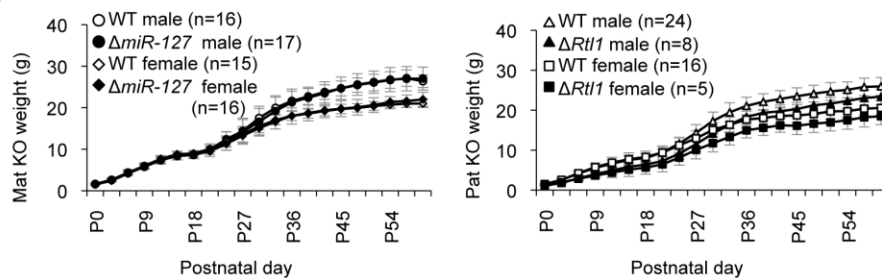
Figures

A
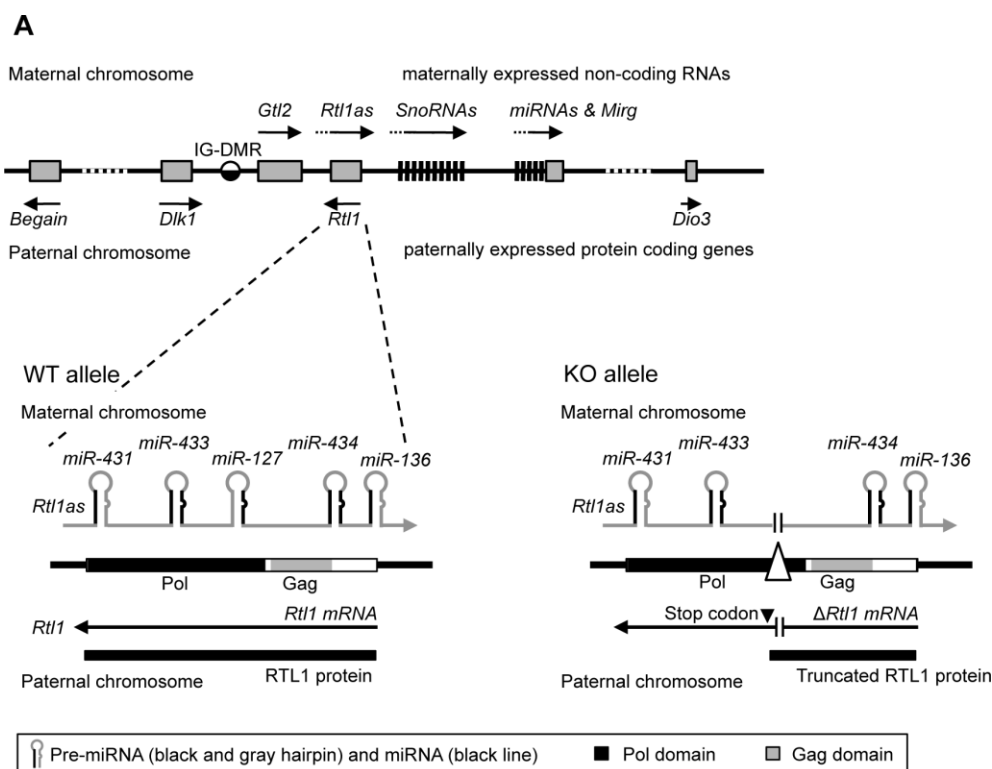
B

C

D

Student's t-test was used for statistic analysis . *** P<0.005
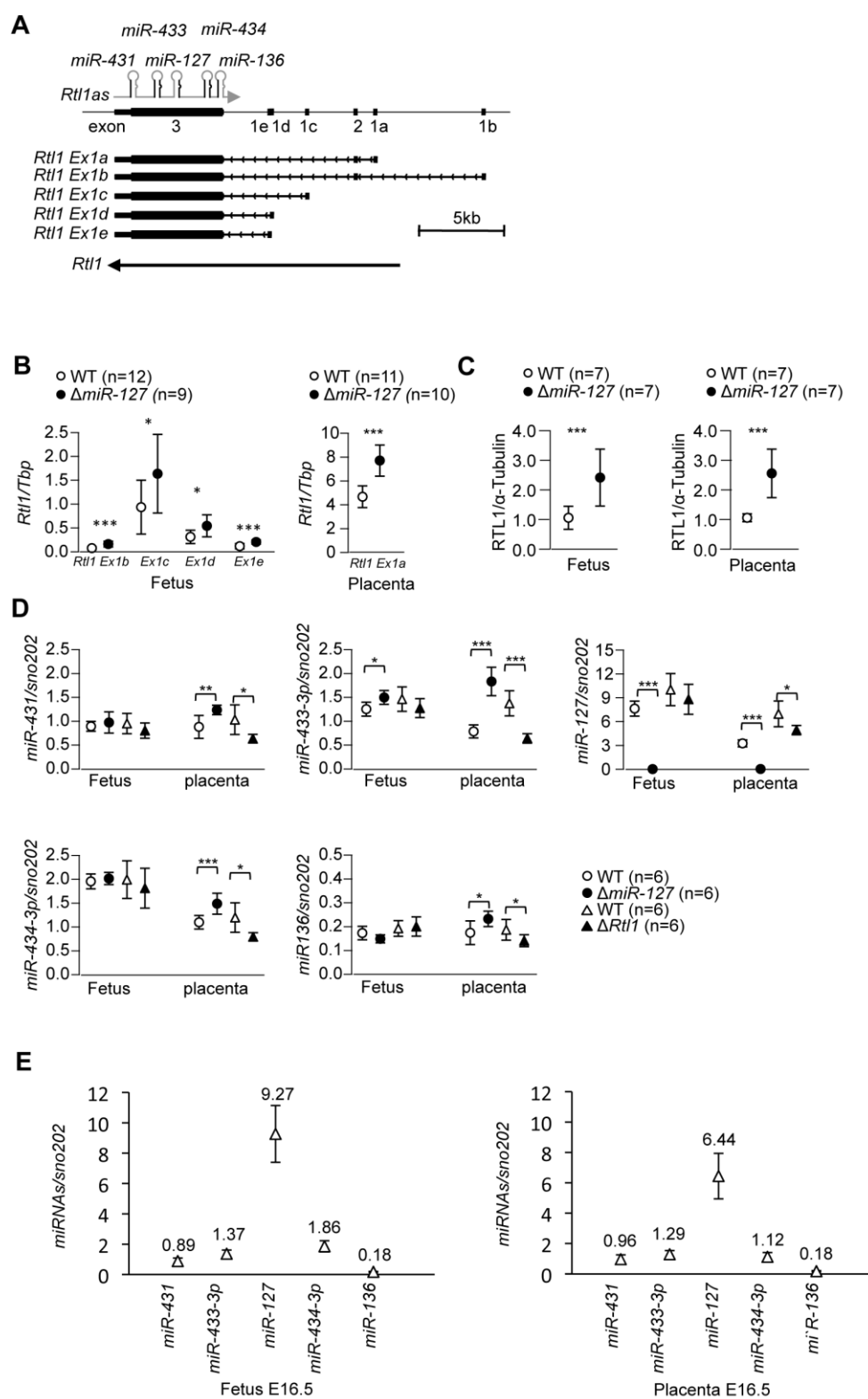Error bars represent SD.

Fig. 1. Structure of *Rtl1* locus and pre- and postnatal growth of *miR-127* KO and *Rtl1* KO mice. (A) Schematic presentation of the *Dlk1-Dio3* cluster. Lower left schematic - representation of the WT *Rtl1* locus (Exon3). *Rtl1* is expressed from paternal chromosome and *Rtl1as* is exclusively transcribed from maternal chromosome. Lower right schematic - representation of the knockout allele. The paternal transmitted deletion induces a stop codon in the frame that results in premature termination of RTL1. The maternal transmitted deletion lacks *miR-127* expression. (B, C) Prenatal growth of Δ*miR-127* mice and Δ*Rtl1* mice, respectively. Left and right panels show embryonic and placental growth curves in mutant and WT littermates from E12.5 to E18.5. All embryos and placentas were collected from the N6 and N7 generation. (D) Postnatal growth curve of Δ*miR-127* (left) and Δ*Rtl1* (right) from birth to 2 months. Weights were measured every three days. Δ*Rtl1* mice were significantly smaller than WT.
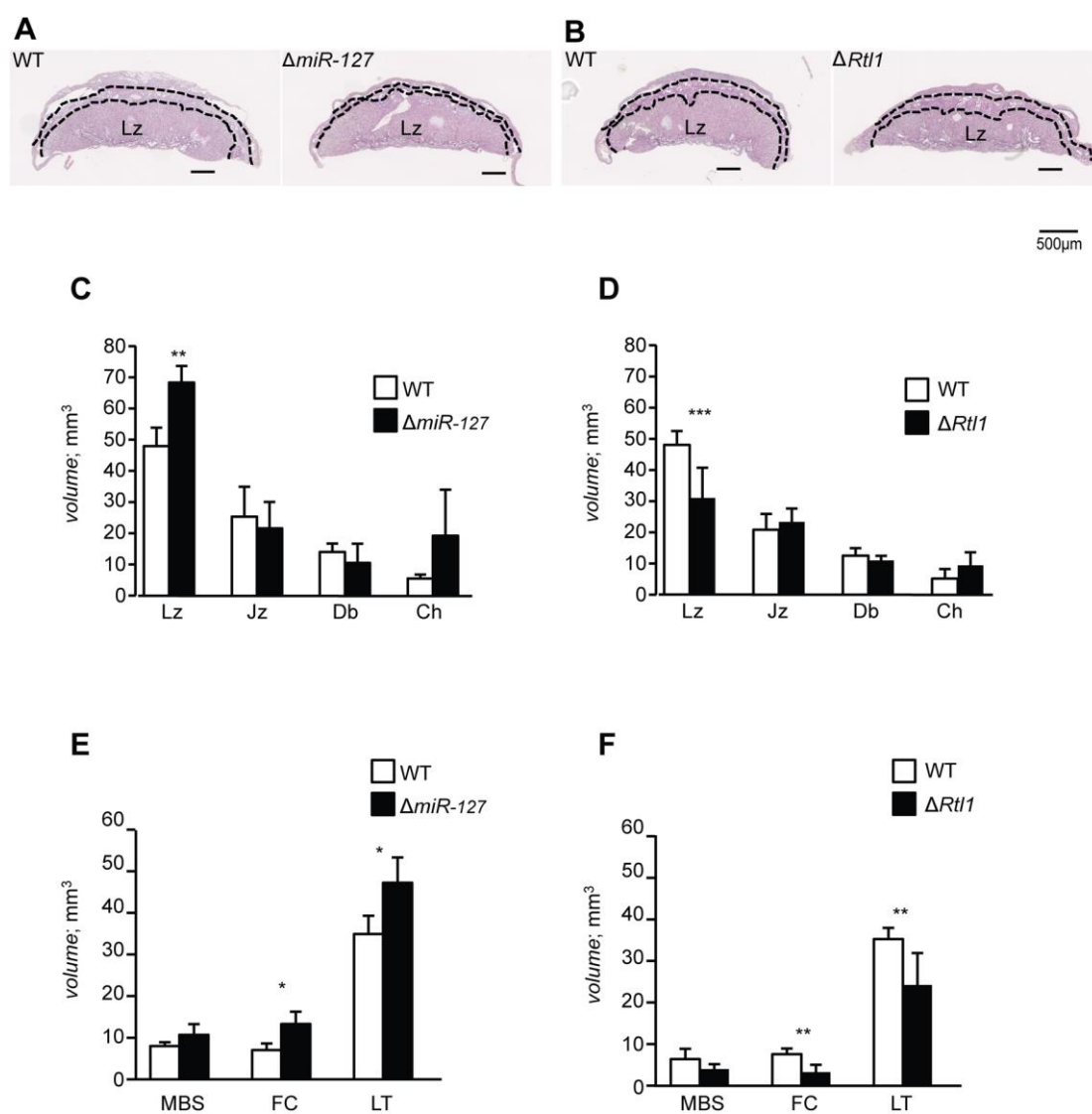
**Fig. 2. Histological analysis shows abnormality in labyrinthine zone in Δ*miR-127***

and Δ*Rtl1*. (A, B) Histological analysis of WT littermate and Δ *miR-127* or Δ *Rtl1*,

respectively. Panels show H&E-stained paraffin sections of E18.5 placentae. (C to F)

The volumes of placental and labyrinthine compartments are indicated.

Student's t-test was used for statistic analysis. * P<0.05, ** P<0.01, *** P<0.005
Error bars represent SD.

Fig. 3. Expression of *Rtl1* alternative transcripts and miRNAs in embryo and placenta at E16.5. (A) Structure of the *Rtl1* locus. Alternative transcripts are transcribed from different leader exons. Exon1s are named 1a-1d. All alternative transcripts have common exon3 that has a conserved retrotransposon sequence. *Rtl1 Ex1a* and *Ex1b* also have common exon2. Exons are represented as solid bar. (B) Quantitative expression analysis for each alternative *Rtl1* transcript in ΔmiR-127 embryo and placenta at E16.5. (C) Western Blotting for RTL1 normalized to α-TUBULIN in Δ*miR-127* embryo and placenta at E16.5. (D) miRNAs expression is shown normalized to *snoRNA202*. (E) The relative expression of miRNAs. *miR-127* is most abundant miRNA among other miRNAs in *Rtl1as*.
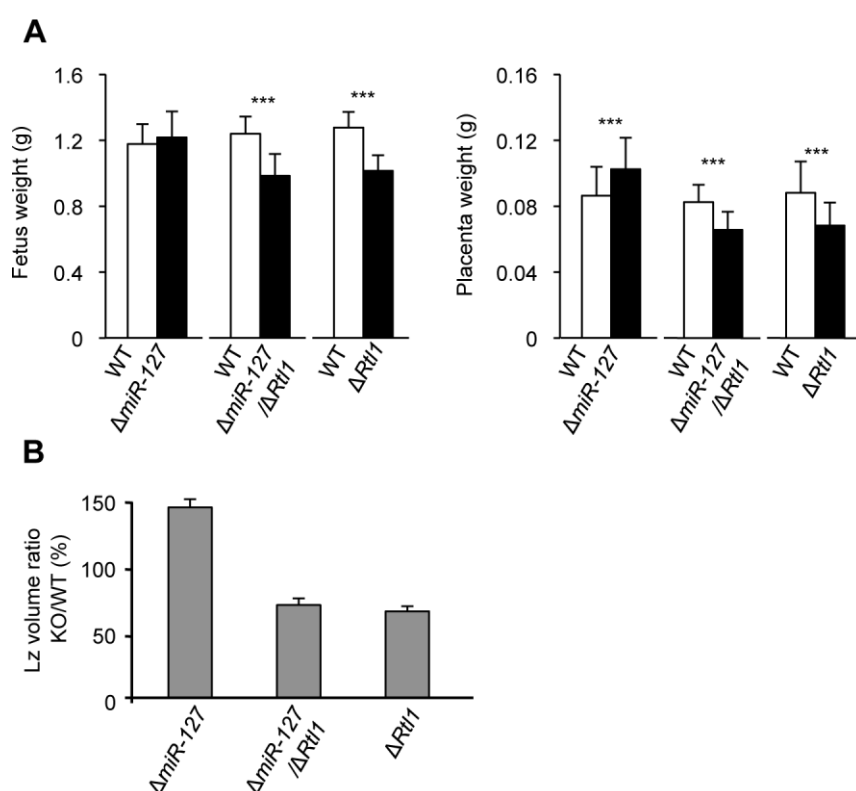
Fig. 4. Δ*miR-127*/Δ*Rtl1* KO mice are comparable to Δ*Rtl1*. Double heterozygous mice carrying both Δ*miR-127* and Δ*Rtl1* were born from heterozygous parents. (A) Fetal and placental weights at E18.5 are shown. (B) Volumes ratio of the placental Lz at E18.5.